A Dynamically Consistent Numerical Approach for the Ebola Virus Transmission Model with Fuzzy Parameters and Time Delay

Muhammad Tashfeen[1], Fazal Dayan[1], Muhammad Aziz ur Rehman[1], Thabet Abdeljawad[2,3,4,5,*] and Bahaaeldin Abdalla[2]

[1] Department of Mathematics, School of Science, University of Management and Technology, Lahore, 54000, Pakistan

[2] Department of Mathematics and Sciences, Prince Sultan University, Riyadh, 11586, Saudi Arabia

[3] Department of Medical Research, China Medical University, Taichung, 40402, Taiwan

[4] Department of Mathematics and Applied Mathematics, School of Science and Technology, Sefako, Makgatho Health Sciences University, Ga-Rankuwa, 0208, South Africa

[5] Center for Applied Mathematics and Bioinformatics (CAMB), Gulf University for Science and Technology, Hawally, 32093, Kuwait

INFORMATION

Keywords:
Ebola virus
delayed epidemic model
fuzzy parameters
stability
numerical algorithms
non-standard finite difference scheme
sensitivity

DOI: 10.23967/j.rimni.2024.10.56870

SCIPEDIA Revista Internacional de Métodos Numéricos para Cálculo y Diseño en Ingeniería

Revista Internacional Métodos numéricos para cálculo y diseño en ingeniería RIMNI CIMNE

A Dynamically Consistent Numerical Approach for the Ebola Virus Transmission Model with Fuzzy Parameters and Time Delay

Muhammad Tashfeen[1], Fazal Dayan[1], Muhammad Aziz ur Rehman[1], Thabet Abdeljawad[2,3,4,5,*] and Bahaaeldin Abdalla[2]

[1]Department of Mathematics, School of Science, University of Management and Technology, Lahore, 54000, Pakistan

[2]Department of Mathematics and Sciences, Prince Sultan University, Riyadh, 11586, Saudi Arabia

[3]Department of Medical Research, China Medical University, Taichung, 40402, Taiwan

[4]Department of Mathematics and Applied Mathematics, School of Science and Technology, Sefako, Makgatho Health Sciences University, Ga-Rankuwa, 0208, South Africa

[5]Center for Applied Mathematics and Bioinformatics (CAMB), Gulf University for Science and Technology, Hawally, 32093, Kuwait

ABSTRACT

The Ebola virus disease (EVD) is a major threat to human health, especially in Central West Africa. In this study, the transmission dynamics of EVD infection are studied using the Susceptible, Infected, Recovered, Deceased, and Pathogen (SIRDP) epidemic framework that prioritizes identifying and quantifying the sources of uncertainty in parameters. Conventional quantitative methods may believe that all measurements are exact, but in reality, data can often be imprecise or hard to measure. To overcome this challenge, fuzzy theory has been integrated into the model due to its flexibility in managing uncertainty. Additionally, this study considers the temporal dynamics of EVD transmission by integrating time delays, which makes the model fit the real-world simulation of disease progression. A sensitivity analysis of the reproductive number was also conducted to assess the impact of key parameters on the transmission dynamics. The behavior of the model has been numerically explored using various algorithms, such as the forward Euler method and the Non-Standard Finite Difference (NSFD) scheme. Some significant numerical characteristics like positivity, convergence, and consistency have been assessed, which indicates that the NSFD method can capture the trends of EVD with fuzzy parameters. The proposed scheme maintains important characteristics of the traditional epidemic models and provides a stable approach for assessing EVD patterns in conditions of risks and unknown variables. The computational experiment confirms the theoretical conclusions and depicts the deficiencies of the normal finite difference approximations, notably for large step sizes, and supports the advantages of the NSFD approach in maintaining the structure of the model.

OPEN ACCESS

Received: 01/08/2024

Accepted: 16/10/2024

DOI
10.23967/j.rimni.2024.10.56870

Keywords:
Ebola virus
delayed epidemic model
fuzzy parameters
stability
numerical algorithms
non-standard finite difference scheme
sensitivity

*Correspondence: Thabet Abdeljawad (tabdeljawad@psu.edu.sa). This is an article distributed under the terms of the Creative Commons BY-NC-SA license

1 Introduction

Mathematical modeling explains the transmission patterns of infectious diseases and provides acceptable approaches to control them, which, hence, becomes a crucial tool for dealing with their complex dynamics. It helps researchers explain how infectious diseases spread in populations. These models consider population size, disease incubation periods, contact networks, and intervention strategies. They are used to predict how an outbreak will develop and evaluate treatments' effectiveness. The susceptible-infectious-recovered (SIR) model, along with its variants, provides an organized framework for analyzing diseases such as Influenza, Measles, and COVID-19. With the power of predicting the epidemic trajectories and analyzing the treatments' success, mathematical modeling provides a strong base for policymakers to make informed and reliable decisions. To achieve better performance, various strategies are developed using different control measures like social distancing and vaccination rates. These adjusted values help address practical issues such as implementing public health interventions, managing resources effectively, and preventing the spread of infectious diseases. Mathematical modeling also finds the most suitable values for control parameters to prevent disease transmission. Hence, it makes it possible to design a personalized strategy to manage the epidemic effectively. Mathematical modeling in epidemiology originated around 1760, highlighted by Daniel Bernoulli's research on smallpox epidemiology [1]. In 1911, Ross [2] analyzed malaria transmission dynamics. Kermack et al. [3] presented a compartmental epidemic model that analyzes the proportionality between infection and one's vulnerability. Various infectious diseases, including influenza, hepatitis, Zika, measles, tuberculosis, malaria, and recently examined COVID-19, are the most attention-grabbing problems related to public health [4–6]. Mathematical epidemiology proved its worth in predicting effective solutions to the health mentioned above issue. Dengue models as susceptible infected recovered-susceptible infected (SIR-SI) show that inter-compartment interactions could be reduced by increasing the awareness rate [7]. Susceptible, vaccinated, exposed, infected, and recovered (SVEIR) models assume that vaccinated people should be in a better position regarding information on past epidemics than those in the susceptible class. Experts should use models and data to supplement their determinations to derive as much useful information as possible when approaching critical decision-making [8]. Kermack and McKendrick's model provides a basis for designing more effective epidemic models, including SI, SIR, and SVEIR. These models can deal with certain important features, such as the risk of recovered patients getting infected again and the effect of awareness and memory on disease dynamics [9].

Delayed epidemic models are mathematical representations of an epidemic that include transmission delays or response delays related to an epidemic. Misra et al. [10] studied different ways of introducing delays and using exposed populations. They also analyzed the steady states with stability and characteristics of the models to detect when those models can predict an epidemic. Concerning these motivations, oscillations, changes in time derivatives, non-uniqueness and stability are the different alternatives for these models. Nonetheless, the dynamics may be altered due to delays [11]. Much research is devoted to epidemics or modeling disease transmission using delay differential equations (DDEs) [12,13]. Maturation periods, the time taken by a vaccine to become effective, the incubation stage, and the recovery period are frequently used by researchers when considering models based on DDEs. Meziane et al. [14] investigated epidemic models of two viruses or viral strain delays. Ghosh et al. [15] used the mean value of disease duration as a delay parameter to introduce a time lag in recovery and mortality rates. The epidemic properties of the delay model were calculated, and a numerical comparison was conducted between the distributed model, delay model, and standard SIR model. Almuqati et al. [16] studied the framework of a multi-group epidemic model considering the effect of logistic growth and delay time distribution. Temporal delay-based models are investigated

by researchers [17]. Discrete and distributed delays are two variants of delay [18]. Tipsri et al. [19] investigated the local stability of both endemic and disease-free equilibria in an SEIR epidemic model with a nonlinear incidence rate and time delay. Hussien et al. [20] determined how epidemic dynamics within the prey population were affected by the delay time and how the presence of infection in the prey population influenced the behavior of the model. Shatanawi et al. [21] examined the fractional dynamics of the tuberculosis (TB) model. Alkhazzan et al. [22] analyzed a novel epidemic model for two diseases incorporating treatment functions. Moreover, mathematical analysis and numerical simulations of the piecewise dynamics model of Malaria transmission are studied by [23]. Din et al. [24] analyzed a stochastic hepatitis B model considering a time delay in the transmission coefficient. A Bifurcation analysis of a delayed stochastic hepatitis B virus (HBV) was presented by [25].

Fuzzy variables express the inherent ambiguity and variability in real-world epidemic dynamics. Various fields of life, such as engineering, meteorology, manufacturing, medicine, promotion decisions, reasoning, and decision-making, use fuzzy set theory [26,27]. The uncertainties and impreciseness inherent in epidemic data and control parameters are analyzed using fuzzy mathematical models. These models use fuzzy sets and numbers to describe epidemiological factors like transmission and recovery rates. The main source of fuzziness derives from the basic language, where the interpretations of undertakings are ill-defined. For instance, when making a statement about an illness in a particular community, the statement may not be black or white, which means it may not be right or wrong but may be right in part. Thus, vagueness should be used as the basis for increasing cognition. This theoretical fuzziness can be mapped to fuzzy sets, which allow a degree to each set member, which is a measure of membership. The fusion of fuzzy sets, logic, and mathematical modeling positively affected different academic fields such as social sciences, scientific disciplines, and epidemiology. Such use of fuzzy sets and logic could be witnessed in literature as Abdy et al. [28], Li et al. [29], Shi et al. [30], and Stiegelmeier et al. [31], among others. The effectiveness of an Non-Standard Finite Difference (NSFD) approach in capturing disease dynamics and supporting decision-making for control strategies was also demonstrated. Dayan et al. [32] discussed a susceptible, infectious. They recovered (SIR) model in a fuzzy environment that showed uncertainty because of the different levels of vulnerability, infectivity, and recovery among infected in a certain population. In light of the above contributions, this research proposes a model of amoebiasis infection in a fuzzy environment. Using fuzziness, the fuzzy SEIR Amoebiasis model was presented with equilibrium analysis and reproductive number assessment by Alqarni et al. [33].

The Ebola virus disease (EVD), first identified in Africa, is a rare and potentially fatal disease that affects both humans and non-human primates. The Ebola virus was first discovered in 1976 near the Ebola River in the Democratic Republic of the Congo. Since then, there have been repeated outbreaks in different African countries [34,35]. EVD infection can cause a fatal hemorrhagic fever, with a mortality rate of approximately 50%–90% if left untreated. Recent outbreaks in Uganda and the Democratic Republic of Congo highlight serious threats to human health. Between 1976 and 2014, at least 18 Ebola outbreaks were confirmed in Africa, with approximately 2400 cases and 1600 deaths by 2012. On 27 March 2014, a new outbreak occurred in West Africa, with 28,602 confirmed cases and 11,301 deaths [36,37]. Reference [38] discussed optimal control of Ebola outbreaks through vaccination restrictions. Two mathematical models were evaluated to understand the ongoing spread of the Ebola virus in West Africa [39]. Ismail et al. [40] studied the Ebola virus, a negative-sense single-stranded RNA virus that is highly contagious and causes lethal EVD. Ebola virus infection remains one of the most serious health threats, causing numerous deaths. Rachah et al. [41] analyzed a simple mathematical model of the Ebola outbreak in Liberia in 2014 and proposed an Ebola compartment model containing eight nonlinear differential equations. Researchers have used

mathematical models to predict the transmission of viruses, including Ebola, between humans. Various classical mathematical approaches have been used to explain the disease caused by EVD, such as the SI model, SIR model, SEIR model, susceptible exposed infected recovered deceased (SEIRD) model, and susceptible exposed infected hospitalized recovered (SEIRHD) model [42,43]. Verma et al. [44] applied this theory to construct SEIR and SEIRHD models for the Ebola epidemic. Ren et al. [45] formulated an EVD model with four transmission modes and a time delay describing the incubation period. Nisar et al. [46] developed a nonlinear fractional order Ebola virus with a novel piecewise hybrid technique to observe the dynamical transmission. Kengne et al. [47] studied an Ebola epidemic model with an exponential nonlinear incidence function that considers efficacy and behavior change. Abbas et al. [48] have developed a modified mathematical model of the Ebola virus, adding the quarantine population as a control strategy. Ko et al. [49] employed a stochastic modeling approach to analyze the spread of EVD during the early stages of an outbreak. Several segmental models of the Ebola epidemic have been proposed [50–54] to mention a few. Noorwali et al. [55] proposed new coincidence point results for single-valued mappings and an L-fuzzy set-valued map in metric spaces. Alazman et al. [56] presented a restricted SIR mathematical model to analyze the evolution of a contagious infectious disease outbreak.

The rest of this paper is organized as follows: Section 2 discusses a mathematical delay model derived from the traditional Ebola virus disease (EVD) model and its subsequent transformation into a fuzzy delayed epidemic model. It also includes equilibrium analysis, calculation of reproduction number, and sensitivity analysis to assess stability. Section 3 presents various numerical schemes, including the Euler order scheme and fuzzy delayed nonstandard finite difference (FDNSFD), and evaluates their certainty, convergence, and consistency. Section 4 contains the numerical simulations, and Section 5 concludes the article.

2 Model Formation

To understand and predict the spread of EVD, we considered the Susceptible, Infected, Recovered, Deceased, and Pathogen (SIRDP) model as introduced by Berge et al. [57], divided the population into five distinct compartments: Susceptible S refers to people vulnerable to getting an EVD; Infected I are people who had contracted the virus and can spread it; Recovered R are persons who have been cured and develop immunity; Deceased D are persons who died from EVD; Pathogen P which represents the concentration of the virus in the environment. More so, the transmission of EVD has multiple routes ranging from direct contact between infected humans and other humans as well as contact with contaminated objects. To model these dynamics, two key elements are incorporated: The other two is time delay τ which is the time taken between the infection of an individual and when it becomes infectious, which plays a significant role in describing the temporal advancement of the disease spread and fuzzy parameters. These parameters are used to control uncertainties and impreciseness obtained from real epidemiological data, and as such, they cope with changes in the model. The corresponding

differential equations for the model are provided below:

$$\begin{cases} \dfrac{dS}{dt} = A - (\beta I + BD + \pi P)S - \mu S, \\ \dfrac{dI}{dt} = (\beta I + BD + \pi P)S - (\mu + \sigma + \gamma)\, I, \\ \dfrac{dR}{dt} = \gamma I - \mu R, \\ \dfrac{dD}{dt} = (\mu + \sigma)\, I - bD, \\ \dfrac{dP}{dt} = \delta + \eta I + \alpha D - \varphi P. \end{cases} \tag{1}$$

The fuzzy model corresponding to the above model is given by:

$$\begin{cases} \dfrac{dS}{dt} = A - (\beta(\upsilon) I + BD + \pi P)S - \mu S, \\ \dfrac{dI}{dt} = (\beta(\upsilon) I + BD + \pi P)S - (\mu + \sigma(\upsilon) + \gamma(\upsilon))\, I, \\ \dfrac{dR}{dt} = \gamma(\upsilon) I - \mu R, \\ \dfrac{dD}{dt} = (\mu + \sigma(\upsilon))\, I - bD, \\ \dfrac{dP}{dt} = \delta + \eta I + \alpha D - \varphi P. \end{cases} \tag{2}$$

The disease transmission rate, mortality rate, and recovery rate for infected individuals are displayed as fuzzy numbers to reflect their inherent uncertainties. We use the membership function used by Bhuju et al. [58]. These parameters are denoted as $\beta(\upsilon)$, $\sigma(\upsilon)$, and $\gamma(\upsilon)$, respectively, and are defined as:

$$\beta(\upsilon) = \begin{cases} 0, & \upsilon \le \upsilon_{min} \\ \dfrac{\upsilon - \upsilon_{min}}{\upsilon_{max} - \upsilon_{min}}, & \upsilon_{min} < \upsilon \le \upsilon_{max} \\ 1, & \upsilon_{max} \le \upsilon \end{cases} \tag{3}$$

where υ_{min} and υ_{max} are the minimum and maximum thresholds of the control variable υ. This piecewise function models how the effectiveness of interventions impacts the transmission rate. The transmission rate $\beta(\upsilon)$ indicates the rate of infection of the susceptible population by contact with the infective persons along with the environmental pathogen. It is a function of the control variable υ, wherein υ might be a function of the intervention such as in the context of sanitation drives or public awareness initiatives.

The mortality rate $\sigma(\upsilon)$ denotes the rate of the deaths of such persons identified with the disease. This rate depends on υ, which captures the impact of other parameters such as virus pathogenicity

and other measures as regards mortality.

$$\sigma(\upsilon) = \begin{cases} \dfrac{(1-\xi)-a_0}{\upsilon_{min}}\upsilon + a_0, & 0 \le \upsilon \le \upsilon_{min} \\ 1-\xi, & \upsilon_{min} < \upsilon \end{cases} \tag{4}$$

Here, a_0 is the mortality rate in the absence of any interventions, intervention being defined as an action, program, or measure that is taken to alter an existing condition or state. Here, ξ denotes the constructs that mitigate recovery effectiveness, including the level of virulence of the virus or lack of available healthcare facilities. As υ increases, meaning that the implemented interventions are effective, $\sigma(\upsilon)$ reduces hence lowering mortality.

The parameter $\gamma(\upsilon)$ stands for the recovery rate, which depicts the rate at which the number of infected individuals recover from the disease. It rises with interventions that have been well coordinated.

$$\gamma(\upsilon) = \frac{(\gamma_0 - 1)}{\upsilon_{max}}\upsilon + 1. \quad 0 \le \upsilon \le \upsilon_{max}. \tag{5}$$

Here, γ_0 represents the maximum recovery rate when no actions are taken. As the effectiveness of interventions rises, so does υ. In addition, γ_0 also rises, this denotes that the recovery rate is higher.

2.1 Fuzzy Delayed Model

Delayed epidemic models are important for understanding and predicting the dynamics of infectious diseases when there is a large incubation period between infection and the onset of infectivity. The symbol τ stands for the incubation period, which indicates the time it takes for an infected person to become contagious. Including $e^{-\mu\tau}$ assumes a linear decline in the population over this period and takes into account factors such as mortality and recovery determined by $\mu\tau$. By including the $(t-\tau)e^{-\mu\tau}$ factor in the susceptible and exposed population compartments, the standard fuzzy epidemic model is transformed into a fuzzy delayed epidemic model.

The proposed fuzzy delayed epidemic model of EVD is given below:

$$\begin{cases} \dfrac{dS}{dt} = A - (\beta(\upsilon)I + BD + \pi P)S(t-\tau)e^{-\mu\tau} - \mu S, \\ \dfrac{dI}{dt} = (\beta(\upsilon)I + BD + \pi P)S(t-\tau)e^{-\mu\tau} - (\mu + \sigma(\upsilon) + \gamma(\upsilon))\, I, \\ \dfrac{dR}{dt} = \gamma(\upsilon)I - \mu R, \\ \dfrac{dD}{dt} = (\mu + \sigma(\upsilon))\, I - bD, \\ \dfrac{dP}{dt} = \delta + \eta I + \alpha D - \varphi P. \end{cases} \tag{6}$$

2.2 *The Fuzzy Basic Reproductive Number (BRN) ($\mathcal{R}_0^f$)*

The BRN number $\mathcal{R}_0$ is calculated by utilizing the next-generation approach

$$\mathcal{R}_0 = \frac{Ae^{-\mu\tau}(b\beta(\upsilon) + B(\mu + \sigma(\upsilon)) + \pi A(b\eta + \alpha\sigma(\upsilon) + \alpha\mu)}{b\mu(\mu + \sigma(\upsilon) + \gamma(\upsilon))}, \tag{7}$$

$$\mathcal{R}_0 = \frac{Ae^{-\mu\tau}(b\beta(\upsilon) + B(k_2) + \pi A(b\eta + \alpha\sigma(\upsilon) + \alpha\mu)}{b\mu k_1}.$$

where $k_1 = (\mu + \sigma(\upsilon) + \gamma(\upsilon))$ and $k_2 = (\mu + \sigma(\upsilon))$.

The FBRN number $\mathcal{R}_0^f$ can be analyzed as below:

Case 1: If $\upsilon \leq \upsilon_{min}$, then $\beta(\upsilon) = 0$ and we obtain

$$\mathcal{R}_0 = \frac{Ae^{-\mu\tau}(B(k_2) + \pi A(b\eta + \alpha\sigma(\upsilon) + \alpha\mu)}{b\mu k_1}.$$

Case 2: *If* $\upsilon_{min} < \upsilon \leq \upsilon_{max}$, we have $\beta(\upsilon) = \dfrac{\upsilon - \upsilon_{min}}{\upsilon_{max} - \upsilon_{min}}$ and we obtain

$$\mathcal{R}_0 = \frac{Ae^{-\mu\tau}(b\beta(\upsilon) + B(k_2) + \pi A(b\eta + \alpha\sigma(\upsilon) + \alpha\mu)}{b\mu k_1}.$$

Case 3: *If* $\upsilon_{max} \leq \upsilon$, we have $\beta(\upsilon) = 1$ and we obtain

$$\mathcal{R}_0 = \frac{Ae^{-\mu\tau}(b + B(k_2) + \pi A(b\eta + \alpha\sigma(\upsilon) + \alpha\mu)}{b\mu k_1}.$$

Now, $\mathcal{R}_0(\upsilon)$ can be written as

$$\mathcal{R}_0(\upsilon) = \left(\frac{Ae^{-\mu\tau}(B(k_2) + \pi A(b\eta + \alpha\sigma(\upsilon) + \alpha\mu)}{b\mu k_1}, \frac{Ae^{-\mu\tau}(b\beta(\upsilon) + B(k_2) + \pi A(b\eta + \alpha\sigma(\upsilon) + \alpha\mu)}{b\mu k_1}, \frac{Ae^{-\mu\tau}(b + B(k_2) + \pi A(b\eta + \alpha\sigma(\upsilon) + \alpha\mu)}{b\mu k_1}\right).$$

The fuzzy reproductive number can be written as [59]

$$\mathcal{R}_0^f = E[\mathcal{R}_0(\upsilon)],$$

$$\mathcal{R}_0^f = \frac{Ae^{-\mu\tau}\pi A(b\eta + \alpha\sigma(\upsilon) + \alpha\mu)(3B(k_2) + 2b\beta(\upsilon) + b + 4)}{4b\mu k_1}. \tag{8}$$

2.3 *Sensitivity Analysis of* $\mathcal{R}_0$

The suggested EVD model is investigated using sensitivity analysis to see how different factors impact the disease's dynamics. Sensitivity analysis gives information on the impact of each parameter on the spread of Ebola. Identifying the parameters that can be easily modified without significantly disrupting the model's behavior is essential for developing targeted public health strategies. Furthermore, understanding the sensitivity helps target public health interventions, such as improving isolation practices or enhancing recovery rates, to effectively control outbreaks. The sensitivity index

of a parameter is defined as [60]

$$\zeta(\upsilon) = \frac{\varrho}{R_o} \times \frac{\partial}{\partial \varrho}(R_o),$$

where ζ denotes the sensitivity of the parameter ϱ. We calculate the sensitivity of $\beta(\upsilon)$ as

$$\zeta(\beta(\upsilon)) = \frac{\beta(\upsilon)}{R_o} \times \frac{\partial}{\partial \beta(\upsilon)}(R_o) = \frac{b\beta(\upsilon)}{(b\beta(\upsilon) + B(k_2) + \pi A(b\eta + \alpha\sigma(\upsilon) + \alpha\mu)},$$

Similarly,

$$\zeta(A) = \frac{A}{R_o} \times \frac{\partial}{\partial A}(R_o) = 1 + \frac{\pi(b\eta + \alpha\sigma(\upsilon) + \alpha\mu)}{(b\beta(\upsilon) + B(k_2) + \pi A(b\eta + \alpha\sigma(\upsilon) + \alpha\mu)},$$

$$\zeta(B) = \frac{B}{R_o} \times \frac{\partial}{\partial B}(R_o) = \frac{Bk_2}{(b\beta(\upsilon) + B(k_2) + \pi A(b\eta + \alpha\sigma(\upsilon) + \alpha\mu)},$$

$$\zeta(b) = \frac{b}{R_o} \times \frac{\partial}{\partial b}(R_o) = \frac{\beta(\upsilon) + \pi A\eta - b\beta(\upsilon) - B(k_2) - \pi A(b\eta + \alpha\sigma(\upsilon) + \alpha\mu}{(b\beta(\upsilon) + B(k_2) + \pi A(b\eta + \alpha\sigma(\upsilon) + \alpha\mu)},$$

$$\zeta(\alpha) = \frac{\alpha}{R_o} \times \frac{\partial}{\partial \alpha}(R_o) = \frac{\alpha\pi k_2}{(b\beta(\upsilon) + B(k_2) + \pi A(b\eta + \alpha\sigma(\upsilon) + \alpha\mu)},$$

$$\zeta(\gamma(v)) = \frac{\gamma(v)}{R_o} \times \frac{\partial}{\partial \gamma(v)}(R_o) = -\frac{\gamma(v)}{k_1},$$

$$\zeta(\sigma(v)) = \frac{\sigma(v)}{R_o} \times \frac{\partial}{\partial \sigma(v)}(R_o) = \frac{\beta(\upsilon) + \pi A\eta - b\beta(\upsilon) - B(k_2) - \pi A(b\eta + \alpha\sigma(\upsilon) + \alpha\mu}{(b\beta(\upsilon) + B(k_2) + \pi A(b\eta + \alpha\sigma(\upsilon) + \alpha\mu)},$$

$$\zeta(\pi) = \frac{\pi}{R_o} \times \frac{\partial}{\partial \pi}(R_o) = \frac{\pi A(\pi A(b\eta + \alpha\sigma(\upsilon) + \alpha\mu)}{(b\beta(\upsilon) + B(k_2) + \pi A(b\eta + \alpha\sigma(\upsilon) + \alpha\mu)},$$

$$\zeta(\eta) = \frac{\eta}{R_o} \times \frac{\partial}{\partial \eta}(R_o) = \frac{\eta\pi Ab}{(b\beta(\upsilon) + B(k_2) + \pi A(b\eta + \alpha\sigma(\upsilon) + \alpha\mu)},$$

$$\zeta(\tau) = \frac{\theta}{R_o} \times \frac{\partial}{\partial \theta}(R_o) = -\tau,$$

$$\zeta(\mu) = \frac{\mu}{R_o} \times \frac{\partial}{\partial \mu}(R_o) = \frac{e^{-\mu\tau}(\pi A\alpha - \tau(b\beta(\upsilon) + B(k_2) + \pi A(b\eta + \alpha\sigma(\upsilon) + \alpha\mu)}{(b\beta(\upsilon) + B(k_2) + \pi A(b\eta + \alpha\sigma(\upsilon) + \alpha\mu)}.$$

Fig. 1 provides a sensitivity analysis of the basic reproduction number R_o with respect to various epidemiological parameters. The x-axis lists parameters, and the y-axis exhibits their sensitivity indices, indicating how changes affect R_o. Parameters like $\beta(\upsilon)$, A, and $\sigma(\upsilon)$ and have positive sensitivity indices, meaning an increase in these parameters raises R_o. As $\beta(\upsilon)$ representing the transmission rate, boosts the spread of infection, increasing R_o. Conversely, parameters like τ, $\gamma(v)$ and μ show negative sensitivity indices. μ the death rate, $\gamma(v)$ recovery rate decreases R_o. While increasing τ delay factor also reduces R_o. To better manage the disease spread, it would be helpful to emphasize the parameter with the highest negative sensitivity, that is τ would be the most effective parameter to focus on while also minimizing parameters with high positive sensitivity, such as A and $\beta(\upsilon)$ to lower the R_o.

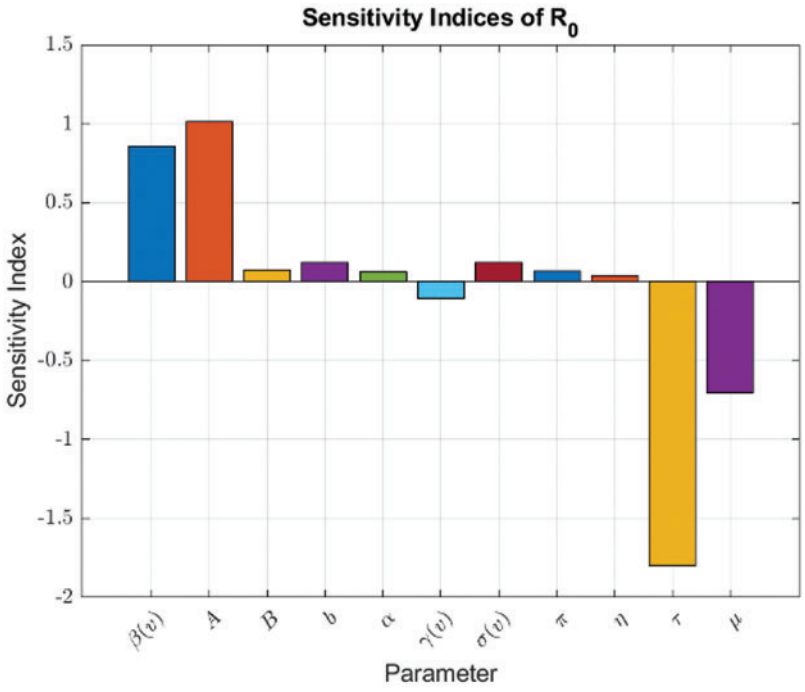

Figure 1: Sensitivity of the basic reproduction number R_o to changes in the model parameters using sensitivity indices

2.4 Equilibrium Analysis

Case 1: If $\upsilon \leq \upsilon_{min}$, we have $\beta(\upsilon) = 0$ and $\mathrm{E}_{\mathrm{p}}^{0}\left(S^0, I^0, R^0, D^0, P^0\right)$, we obtain

$$S^0 = \frac{A}{(BD^0 + \pi P^0)\, e^{-\mu\tau} + \mu),}$$

$$I^0 = \frac{\left(BD^0 + \pi P^0\right) e^{-\mu\tau} S^0}{k_1},$$

$$R^0 = \frac{\gamma(\upsilon) I^0}{\mu},$$

$$D^0 = \frac{k_2 I^0}{b},$$

$$P^0 = \frac{\delta + \eta I^0 + \alpha D^0}{\varphi}.$$

Case 2: If $\upsilon_{min} < \upsilon \leq \upsilon_{max}$, we have $\beta(\upsilon) = \dfrac{\upsilon - \upsilon_{min}}{x_{max} - \upsilon_{min}}$ and $\mathrm{E}_{\mathrm{p}}^{*}(S^*, I^*, R^*, D^*, P^*)$, we obtain

$$S^* = \frac{A}{(\beta(\upsilon) I^* + BD^* + \pi P^*)\, e^{-\mu\tau} + \mu),}$$

$$I^* = \frac{(\beta(\upsilon) I^* + BD^* + \pi P^*) e^{-\mu\tau} S^*}{k_1},$$

$$R^* = \frac{\gamma(\upsilon) I^*}{\mu},$$

$$D^* = \frac{k_2 I^*}{b},$$

$$P^* = \frac{\delta + \eta I^* + \alpha D^*}{\varphi}.$$

Case 3: If $\upsilon_{max} \leq \upsilon$, we have $\beta(\upsilon) = 1$ and $\mathrm{E}_{\mathrm{p}}^{**}(S^{**}, I^{**}, R^{**}, D^{**}, P^{**})$, we obtain

$$S^{**} = \frac{A}{(I^{**} + BD^{**} + \pi P^{**}) e^{-\mu\tau} + \mu)},$$

$$I^{**} = \frac{(I^{**} + BD^{**} + \pi P^{**}) e^{-\mu\tau} S^{**}}{k_1},$$

$$R^{**} = \frac{\gamma(\upsilon) I^{**}}{\mu},$$

$$D^{**} = \frac{k_2 I^{**}}{b},$$

$$P^{**} = \frac{\delta + \eta I^{**} + \alpha D^{**}}{\varphi}.$$

2.5 Stability Analysis

The Jacobian matrix of system (6) at disease free equilibrium (DFE) is given by

$$J(\mathrm{E}_{\mathrm{p}}^0) = \begin{bmatrix} -(BD + \pi P)e^{-\mu\tau} - \mu & 0 & 0 & BDe^{-\mu\tau} & \pi Pe^{-\mu\tau} \\ (BD + \pi P)e^{-\mu\tau} & -k_1 & 0 & 0 & 0 \\ 0 & \gamma & -\mu & 0 & 0 \\ 0 & k_2 & 0 & -b & 0 \\ 0 & \eta & 0 & \alpha & -\varphi \end{bmatrix}.$$

The eigenvalues of the matrix are; $\lambda_1 = -0.500$, $\lambda_2 = -0.0300$, $\lambda_3 = -0.5041$, $\lambda_4 = -0.6105$ and $\lambda_5 = -0.7998$. As all the eigenvalues are less than zero, we concluded that the system of differential equations of the SIRDP model is locally asymptotically stable at $\mathrm{E}_{\mathrm{p}}^0$.

3 Numerical Modelling

Numerical modeling involves simulating and analyzing complex systems or processes using mathematical formulas and computer techniques. This practice provides predictions and insights that cannot be obtained through direct research. Computational techniques and algorithms such as the finite difference method and the finite element method are used to solve the discretized fundamental equations of the system. This section uses a forward Euler scheme and a nonstandard finite-difference method for a particular model.

3.1 Forward Euler Scheme

The forward Euler method is a well-acknowledged explicit first-order numerical methodology for solving ordinary differential equations. It is well-known for its computational efficiency and ability to estimate the trajectory of solutions over time quickly. We construct a forward Euler scheme for the above system (6).

$$S^{n+1} = S^n + hA - h\left(\beta\left(v\right) I^n + BD^n + \pi P^n\right) e^{-\mu\tau} S^n - h\mu S^n, \tag{9}$$

$$I^{n+1} = I^n + h\left(\beta\left(v\right) I^n + BD^n + \pi P^n\right) e^{-\mu\tau} S^n - h\left(\mu + \sigma\left(\upsilon\right) + \gamma\left(\upsilon\right)\right) I^n, \tag{10}$$

$$R^{n+1} = R^n + h\left(\gamma\left(\upsilon\right) I^n - \mu R^n\right), \tag{11}$$

$$D^{n+1} = D^n + h\left(\mu + \sigma(\upsilon)\right) I^n - hbD^n, \tag{12}$$

$$P^{n+1} = P^n + h\left(\delta + \eta I^n + \alpha D^n\right) - h\varphi P^n. \tag{13}$$

3.2 NSFD Scheme

The NSFD method appears to be a computational approach to efficiently solve fuzzy delayed differential equations while maintaining the characteristics of continuous models. Securing positive, stable, and convergent behavior numerical solutions, NSFD schemes [61] are appropriate for dealing with epidemic models. Considering continuous models, NSFD schemes proved their worth over traditional methods, being more efficient and consistent. The proposed fuzzy delayed nonstandard finite difference (FDNSFD) is given by

$$\begin{cases} S^{n+1} = \dfrac{S^n + hA}{1 + h\left(\beta\left(v\right) I + BD^n + \pi P^n\right) e^{-\mu\tau} + h\mu}, \\ I^{n+1} = \dfrac{I^n + h\left(\beta\left(v\right) I + BD^n + \pi P^n\right) e^{-\mu\tau} S^n}{1 + hK_1}, \\ R^{n+1} = \dfrac{R^n + h\gamma(\upsilon) I^n}{1 + h\mu}, \\ D^{n+1} = \dfrac{D^n + hK_2 I^n}{1 + hb}, \\ P^{n+1} = \dfrac{P^n + h(\delta + \eta I^n + \alpha D^n)}{1 + h\varphi}. \end{cases} \tag{14}$$

3.3 Positivity of FDNSFD

Accuracy and relevance are unavoidable parameters when solving epidemic models using numerical methods. In a segmental prevalence model, all variables representing different population segments must have at least one positive value, while other variables may or may not be positive but not always negative. It is important to ensure that these variables are positive. This fundamental property is strictly maintained using principles of mathematical induction within an implicit numerical integration scheme. The following provides valuable insight into this process:

Theorem: Let S, I, R, D and $P \geq 0$ are finite $S + I + R + D + P \leq N$; furthermore, $\alpha \geq 0$, $\delta \geq 0, \mu \geq 0, \gamma(\upsilon) \geq 0, \varphi \geq 0, \sigma(\upsilon) \geq 0, \tau \geq 0, \pi \geq 0$, $B \geq 0, b \geq 0, \eta \geq 0$ and $\beta(v) \geq 0$, then $S^{n+1} \geq 0$, $I^{n+1} \geq 0$, $R^{n+1} \geq 0$, $D^{n+1} \geq 0$ and $P^{n+1} \geq 0$ for all $n \in Z^{+}$.

Proof: Now for $n = 0$ system (14) becomes

$$\begin{cases} S^{1} = \dfrac{S^{0} + hA}{1 + h\left(\beta(v) I + BD^{0} + \pi P^{0}\right) e^{-\mu\tau} + h\mu} \geq 0, \\ I^{1} = \dfrac{I^{0} + h\left(\beta(v) I + BD^{0} + \pi P^{0}\right) e^{-\mu\tau} S^{0}}{1 + hK_{1}} \geq 0, \\ R^{1} = \dfrac{R^{0} + h\gamma(\upsilon)}{1 + h\mu} \geq 0, \\ D^{1} = \dfrac{D^{0} + hK_{2} I^{n}}{1 + hb} \geq 0, \\ P^{1} = \dfrac{P^{0} + h(\delta + \eta I^{0} + \alpha D^{0})}{1 + h\varphi} \geq 0. \end{cases}$$

Now, for $n = 1$ system (14) becomes

$$\begin{cases} S^{2} = \dfrac{S^{1} + hA}{1 + h\left(\beta(v) I + BD^{1} + \pi P^{1}\right) e^{-\mu\tau} + h\mu} \geq 0, \\ I^{2} = \dfrac{I^{1} + h\left(\beta(v) I + BD^{1} + \pi P^{1}\right) e^{-\mu\tau} S^{1}}{1 + hK_{1}} \geq 0, \\ R^{2} = \dfrac{R^{1} + h\gamma(\upsilon)}{1 + h\mu} \geq 0, \\ D^{2} = \dfrac{D^{1} + hK_{2} I^{n}}{1 + hb} \geq 0, \\ P^{2} = \dfrac{P^{1} + h(\delta + \eta I^{1} + \alpha D^{1})}{1 + h\varphi} \geq 0. \end{cases}$$

Assume that the preceding set of equations guarantees that the values of S, I, R, D, and P have the property of positivity for $n = 2, 3, 4, \ldots, n-1$. In other words, for $n = 2, 3, 4, \ldots, n-1$, $S^{n+1} \geq 0, I^{n+1} \geq 0, R^{n+1} \geq 0, D^{n+1} \geq 0$ and $P^{n+1} \geq 0$. The positivity will now be investigated for a random

positive integer n, and we find that

$$\begin{cases} S^{n+1} = \dfrac{S^n + hA}{1 + h\left(\beta\left(v\right) I + BD^n + \pi P^n\right) e^{-\mu\tau} + h\mu} \geq 0, \\ I^{n+1} = \dfrac{I^n + h\left(\beta\left(v\right) I + BD^n + \pi P^n\right) e^{-\mu\tau} S^n}{1 + hK_1} \geq 0, \\ R^{n+1} = \dfrac{R^n + h\gamma\left(\upsilon\right)}{1 + h\mu} \geq 0, \\ D^{n+1} = \dfrac{D^n + hK_2 I^n}{1 + hb} \geq 0, \\ P^{n+1} = \dfrac{P^n + h(\delta + \eta I^n + \alpha D^n)}{1 + h\varphi} \geq 0. \end{cases}$$

Hence, the proof.

3.4 Convergence Analysis

Convergence analysis in epidemic models determines the stability and accuracy of numerical approaches for solving disease-spread differential equations. It determines if the numerical solution approaches the genuine solution when the computational parameters drop, assuring simulation reliability and accuracy while preserving the continuous model's characteristics. To prove this, assume that

$$\begin{cases} Q_1 = \dfrac{S + hA}{1 + h\left(\beta\left(v\right) I + BD + \pi P\right) e^{-\mu\tau} + h\mu}, \\ Q_2 = \dfrac{I + h\left(\beta\left(v\right) I + BD + \pi P\right) e^{-\mu\tau} S}{1 + hK_1}, \\ Q_3 = \dfrac{R + h\gamma\left(\upsilon\right)}{1 + h\mu}, \\ Q_4 = \dfrac{D + hK_2 I}{1 + hb}, \\ Q_5 = \dfrac{P + h(\delta + \eta I + \alpha D)}{1 + h\varphi}. \end{cases}$$

The Jacobian matrix corresponding to the above system at E_p^0 is

$$\mathcal{J}(E_p^0) = \begin{bmatrix} \frac{1}{1+h\mu} & 0 & 0 & 0 & \frac{h\mu}{1+hk_1} \\ 0 & \frac{1}{1+hk_1} & 0 & 0 & 0 \\ 0 & \frac{h\varphi}{1+hk_2} & \frac{1}{1+hk_2} & 0 & 0 \\ 0 & 0 & \frac{h\omega}{1+hk_3} & \frac{1}{1+hk_3} & 0 \\ 0 & 0 & 0 & \frac{h\gamma(x)}{1+hk_4} & \frac{1}{1+hk_4} \end{bmatrix}$$

Eigen values of above Jacobian matrix $\lambda_1 = 0.99700897 < 1$, $\lambda_2 = 0.94255486 < 1$, $\lambda_3 = 0.05087814 < 1$, $\lambda_4 = 0.95238095 < 1$ and $\lambda_5 = 0.95238095 < 1$. All of the Jacobian matrix's eigenvalues will be inside a unit circle, ensuring that the proposed FDNSFD scheme converges at a point E_p^0.

3.5 Consistency of the FDNSFD Scheme

Consistency refers to the ability of a numerical method to accurately estimate the underlying continuous model as factors such as step size are reduced. This result highlights the importance of maintaining the consistency of his FDNSFD system to ensure the reliability and accuracy of numerical solutions.

Beginning with the first equation in the system (14), we get

$$S^{n+1}(1 + h(\beta(v) I + BD^n + \pi P^n) e^{-\mu\tau} + \mu) = S^n + hA, \tag{15}$$

The Taylor's series expansion of the S^{n+1} is as follows:

$$S^{n+1} = \left(S^n + h\frac{dS}{dt} + \frac{h^2}{2!}\frac{d^2S}{dt^2} + \frac{h^3}{3!}\frac{d^3S}{dt^3} + \ldots\right).$$

From Eq. (15), we obtain

$$\left(S^n + h\frac{dS}{dt} + \frac{h^2}{2!}\frac{d^2S}{dt^2} + \frac{h^3}{3!}\frac{d^3S}{dt^3} + \ldots\right)\left(1 + h(\beta(v) I + BD^n + \pi P^n) e^{-\mu\tau} + \mu\right) = S^n + hA.$$

After some simplification and applying $h \to 0$, we get

$$S^n((\beta(v) I + BD^n + \pi P^n) e^{-\mu\tau} + \mu) + \frac{dS}{dt} = A,$$

$$\frac{dS}{dt} = A - (\beta(v) I + BD^n + \pi P^n) S^n e^{-\mu\tau} + \mu S^n,$$

$$\Longrightarrow \frac{dS}{dt} = A - (\beta(\upsilon) I + BD + \pi P) S e^{-\mu\tau} - \mu S.$$

From the second equation of the FDNSFD scheme, we have

$$I^{n+1}(1+hk_1) = I^n + h\left(\beta\left(v\right)I + BD^n + \pi P^n\right)e^{-\mu\tau}S^n, \tag{16}$$

The Taylor's series expansion of the I^{n+1} is as follows:

$$I^{n+1} = \left(I^n + h\frac{dI}{dt} + \frac{h^2}{2!}\frac{d^2I}{dt^2} + \frac{h^3}{3!}\frac{d^3I}{dt^3} + \ldots\right),$$

From Eq. (16), we obtain

$$\left(I^n + h\frac{dI}{dt} + \frac{h^2}{2!}\frac{d^2I}{dt^2} + \frac{h^3}{3!}\frac{d^3I}{dt^3} + \ldots\right)(1+hk_1) = I^n + h\left(\beta\left(v\right)I + BD^n + \pi P^n\right)e^{-\mu\tau}S^n.$$

Apply $h \to 0$, we get

$$I^n k_1 + \frac{dI}{dt} = \left(\beta\left(v\right)I + BD^n + \pi P^n\right)e^{-\mu\tau}S^n,$$

$$\frac{dI}{dt} = \left(\beta\left(v\right)I + BD^n + \pi P^n\right)e^{-\mu\tau}S^n - I^n k_1,$$

$$\Longrightarrow \frac{dI}{dt} = \left(\beta\left(\upsilon\right)I + BD + \pi P\right)Se^{-\mu\tau} - \left(\mu + \sigma\left(\upsilon\right) + \gamma\left(\upsilon\right)\right)I.$$

From the third equation of the FDNSFD scheme, we have

$$R^{n+1}(1+h\mu) = R^n + h\gamma(\upsilon)I^n, \tag{17}$$

The Taylor's series expansion of the R^{n+1} is as follows:

$$R^{n+1} = \left(R^n + h\frac{dR}{dt} + \frac{h^2}{2!}\frac{d^2R}{dt^2} + \frac{h^3}{3!}\frac{d^3R}{dt^3} + \ldots\right),$$

From Eq. (17), we obtain

$$\left(R^n + h\frac{dR}{dt} + \frac{h^2}{2!}\frac{d^2R}{dt^2} + \frac{h^3}{3!}\frac{d^3R}{dt^3} + \ldots\right)(1+h\mu) = R^n + h\gamma(\upsilon)I^n.$$

Apply $h \to 0$, we get

$$\mu R^n + \frac{dR}{dt} = \gamma\left(\upsilon\right)I^n,$$

$$\frac{dR}{dt} = \gamma(\upsilon)I^n - \mu R^n,$$

$$\Longrightarrow \frac{dR}{dt} = \gamma(\upsilon)I - \mu R.$$

From the fourth equation of the FDNSFD scheme, we have

$$D^{n+1}\left(1+hb\right) = D^n + hK_2I^n, \tag{18}$$

The Taylor's series expansion of the I^{n+1} is as follows:

$$D^{n+1} = \left(D^n + h\frac{dD}{dt} + \frac{h^2}{2!}\frac{d^2D}{dt^2} + \frac{h^3}{3!}\frac{d^3D}{dt^3} + \dots\right),$$

From Eq. (18), we obtain

$$\left(D^n + h\frac{dD}{dt} + \frac{h^2}{2!}\frac{d^2D}{dt^2} + \frac{h^3}{3!}\frac{d^3D}{dt^3} + \dots\right)(1+hb) = D^n + hK_2I^n.$$

Apply $h \to 0$, we get

$$bD^n + \frac{dD}{dt} = K_2I^n,$$

$$\frac{dD}{dt} = K_2I^n - bD^n$$

$$\Longrightarrow \frac{dD}{dt} = (\mu + \sigma(\upsilon))I - bD.$$

From the fifth equation of the FDNSFD scheme, we have

$$P^{n+1}(1+h\varphi) = P^n + h(\delta + \eta I^n + \alpha D^n). \tag{19}$$

The Taylor's series expansion of the I^{n+1} is as follows:

$$P^{n+1} = \left(P^n + h\frac{dP}{dt} + \frac{h^2}{2!}\frac{d^2P}{dt^2} + \frac{h^3}{3!}\frac{d^3P}{dt^3} + \dots\right),$$

From Eq. (19), we obtain

$$\left(P^n + h\frac{dP}{dt} + \frac{h^2}{2!}\frac{d^2P}{dt^2} + \frac{h^3}{3!}\frac{d^3P}{dt^3} + \dots\right)(1+h\varphi) = P^n + h\left(\delta + \eta I^n + \alpha D^n\right).$$

Apply $h \to 0$, we get

$$\varphi P^n + \frac{dP}{dt} = \left(\delta + \eta I^n + \alpha D^n\right),$$

$$\frac{dP}{dt} = (\delta + \eta I^n + \alpha D^n) - \varphi P^n,$$

$$\Longrightarrow \frac{dP}{dt} = \delta + \eta I + \alpha D - \varphi P.$$

As a result, the ordinary differential equations (ODEs) above system and our discretized implicit numerical integration technique are consistent.

4 Mathematical Simulations

Table 1 shows the values of the parameters utilized in the numerical simulations.

Table 1: Values of parameters [51]

Parameters	Values	Parameters	Values
A	5	η	0.04
B	0.06	δ	0.01
b	0.8	τ	≥ 0
μ	0.5	$\beta\,(v)$	Fuzzy variable
φ	0.04	$\sigma\,(\upsilon)$	Fuzzy variable
π	0.01	$\gamma\,(\upsilon)$	Fuzzy variable
α	0.05		

Fig. 2 illustrates the infected population at various step sizes using the forward approach. The results indicate non-physical oscillations and negative values, which are not feasible for population compartments.

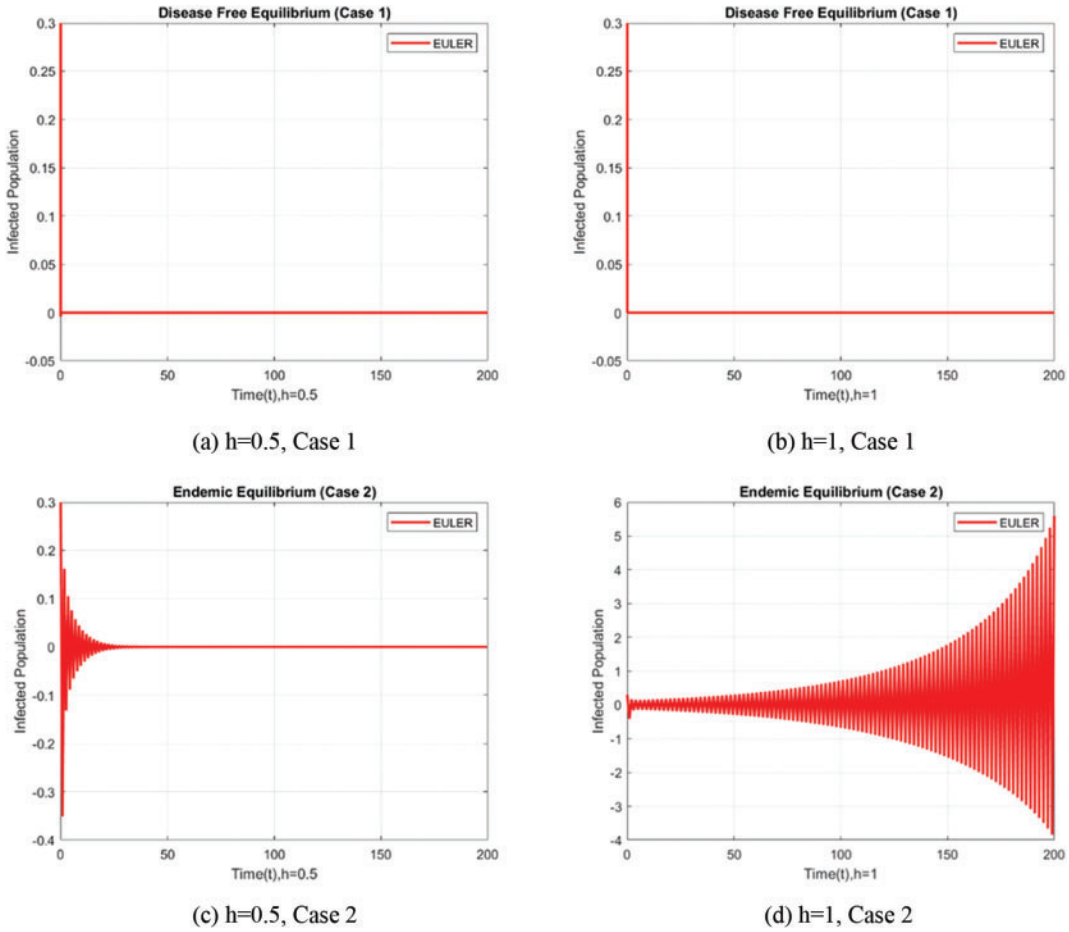

(a) h=0.5, Case 1

(b) h=1, Case 1

(c) h=0.5, Case 2

(d) h=1, Case 2

Figure 2: (Continued)

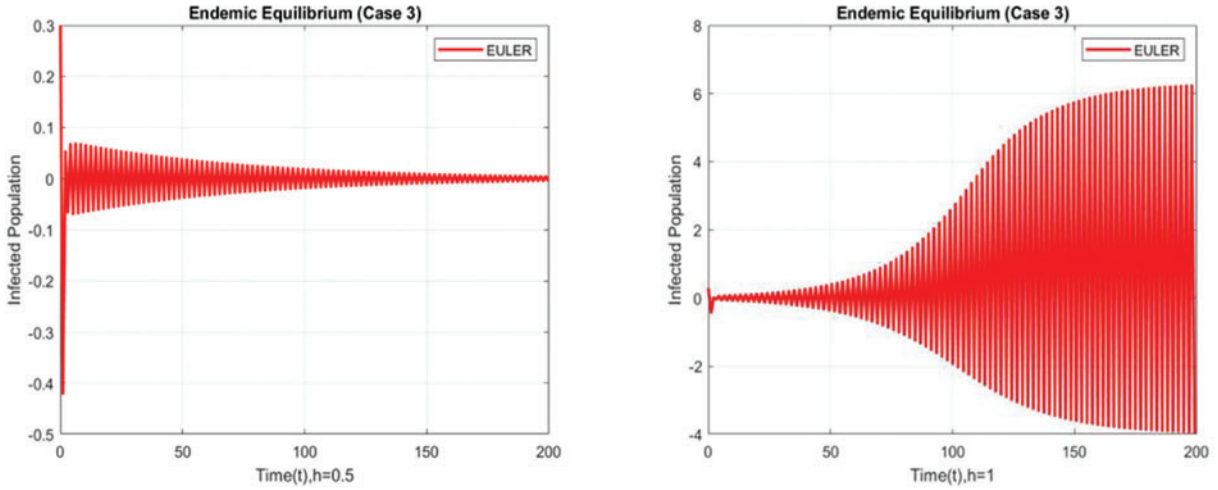

(e) h=0.5, Case 3 (f) h=1, Case 3

Figure 2: Infected population at various step sizes using the forward Euler approach

Fig. 3 presents the behavior of the deceased population, which also demonstrates non-physical oscillations and negative values. This was expected due to the dynamics of the infected population compartments using the forward Euler approach.

Fig. 4 depicts the compartmental behavior of all compartments of the (SIRDP) Ebola virus. It can be observed that the Euler scheme produces nonpositive values and oscillations. Nonpositive values in these models are meaningless as the compartment consists of populations that cannot be negative.

Fig. 5 highlights the behavior of the infected population using the FDNSFD scheme approach for various step sizes. This method preserves positivity and provides the required results.

Fig. 6 shows the deceased populations at various step sizes using the FDNSFD method, yielding almost entirely positive values and results, as observed for the infected population.

Fig. 7 compares all the compartments of SIRDP using the FDNSFD approach. It details the behavior of the infected population for each case during the FDNSFD approach.

Fig. 8 displays the infected population results for each scenario using the FDNSFD approach, showing an increase in the infected population across all cases. Notably, in Case 1, we observe a nearly disease-free state. In contrast, in Cases 2 and 3, an endemic equilibrium state is evident, with Case 3 exhibiting a higher number of infected individuals than Case 2.

Fig. 9 showcases the infected and deceased populations with and without a delay factor, utilizing a fuzzy delayed NSFD model. The graph indicates that implementing a delay factor effectively controls the disease, with fewer individuals infected with the Ebola virus.

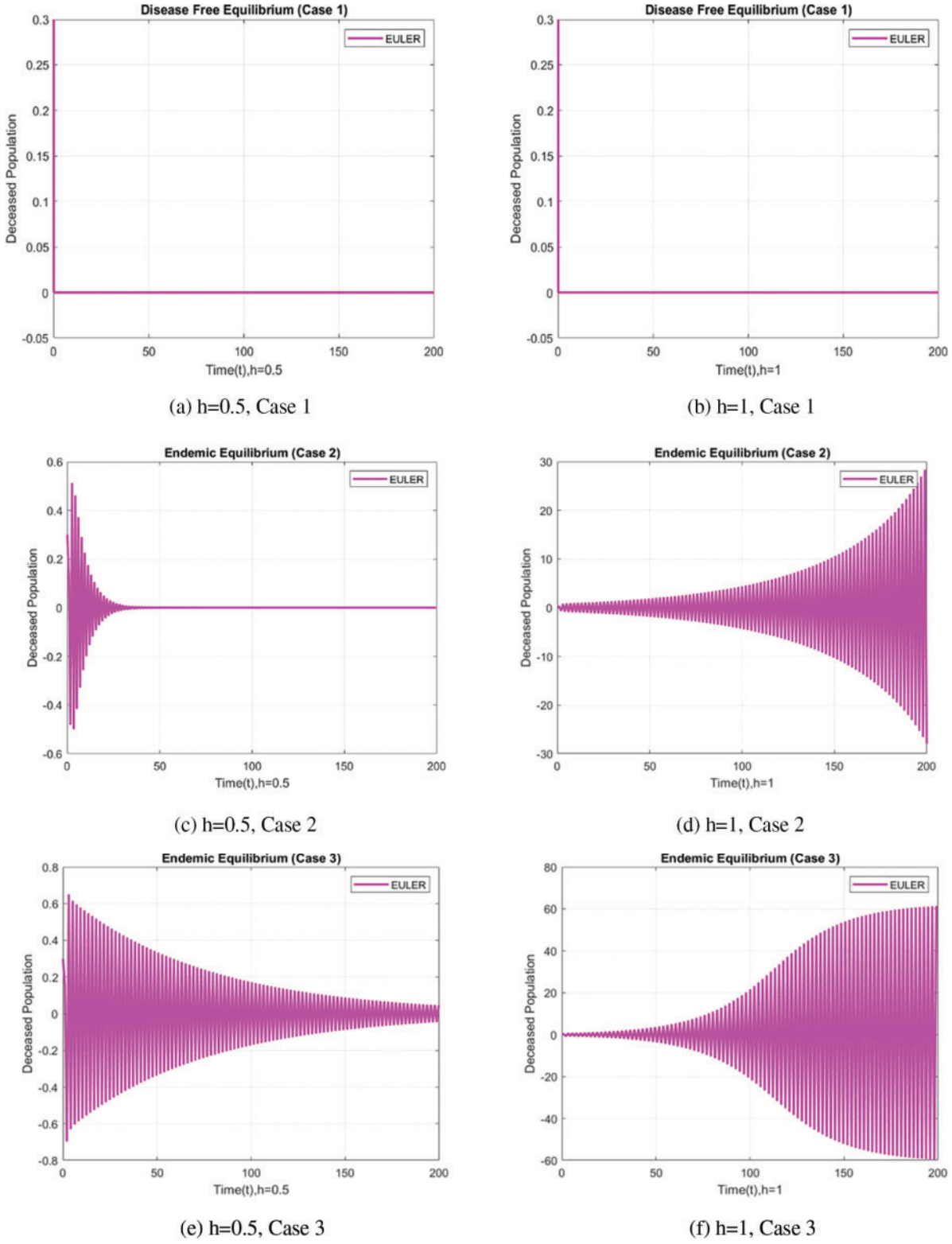

Figure 3: Deceased population at various step sizes using the forward Euler approach

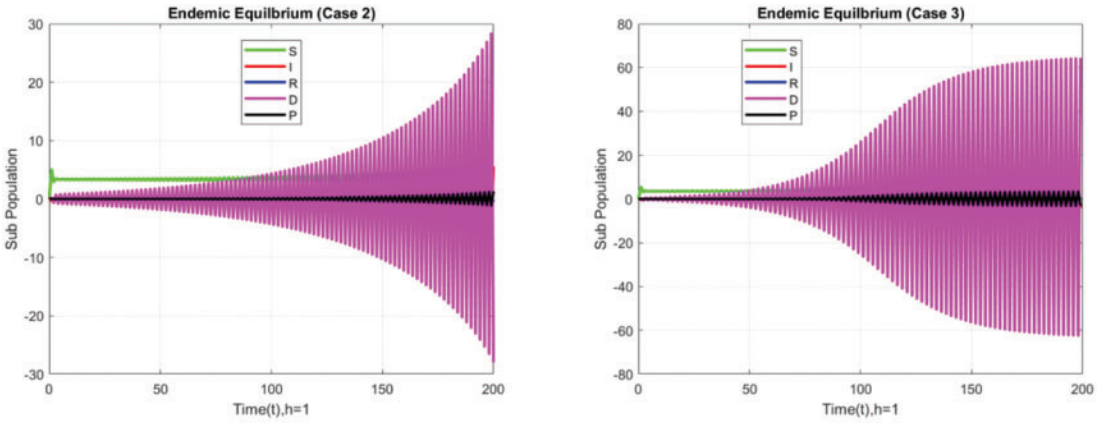

(a) h=1, Case 2 (b) h=2, Case 3

Figure 4: Compartmental comparison of SIRDP using the forward Euler approach

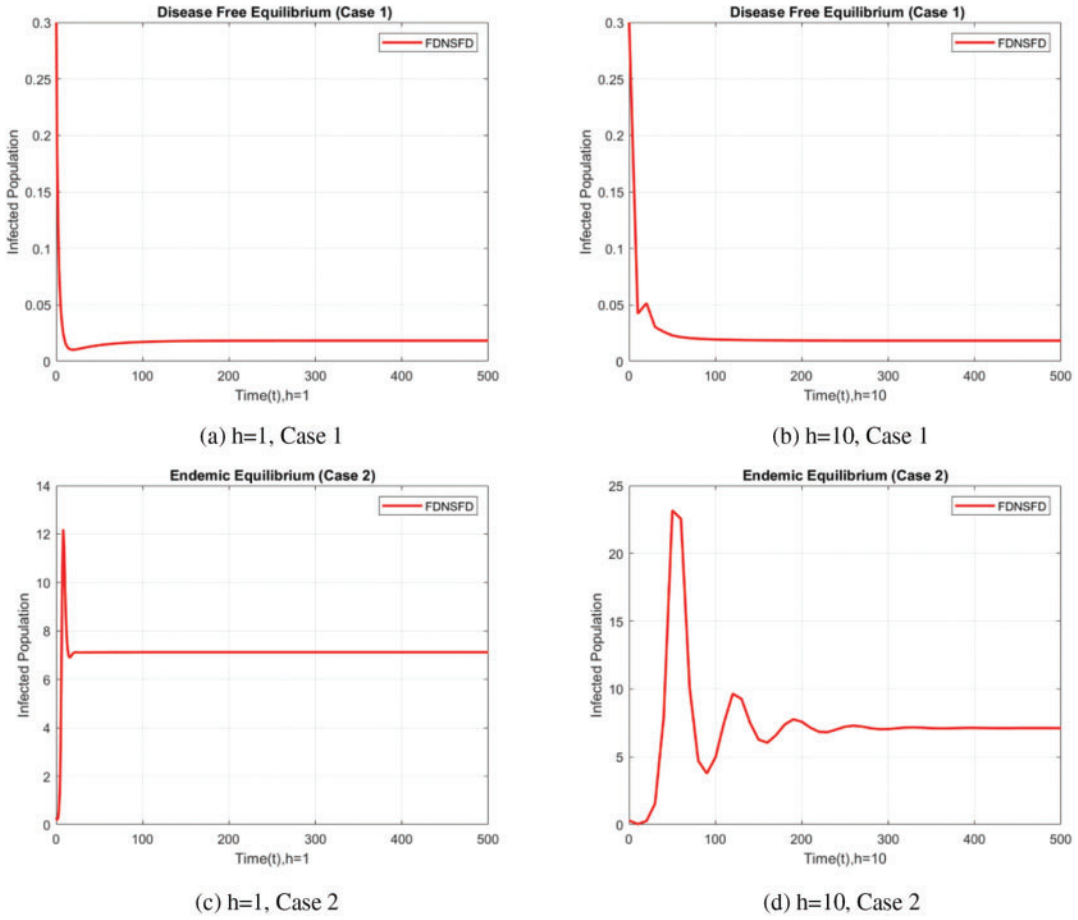

(a) h=1, Case 1 (b) h=10, Case 1

(c) h=1, Case 2 (d) h=10, Case 2

Figure 5: (Continued)

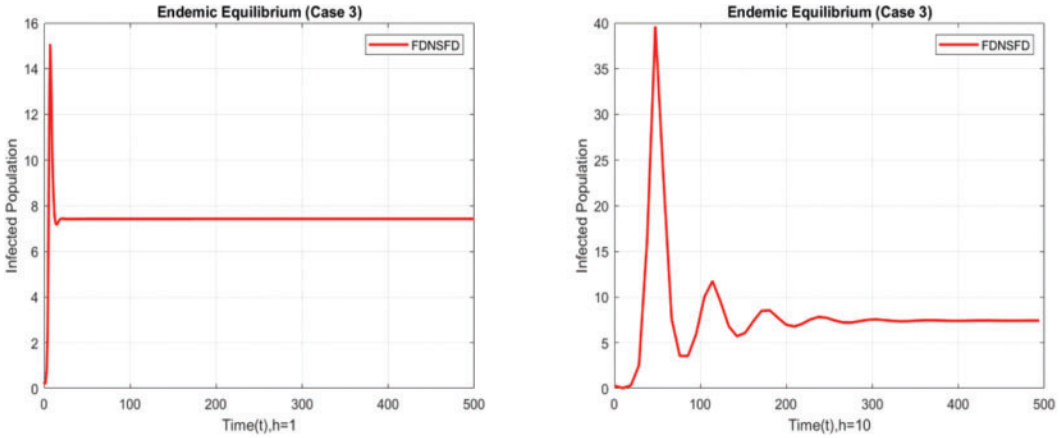

(e) h=1, Case 3 (f) h=10, Case 3

Figure 5: Infected population at various step sizes using the FDNSFD approach

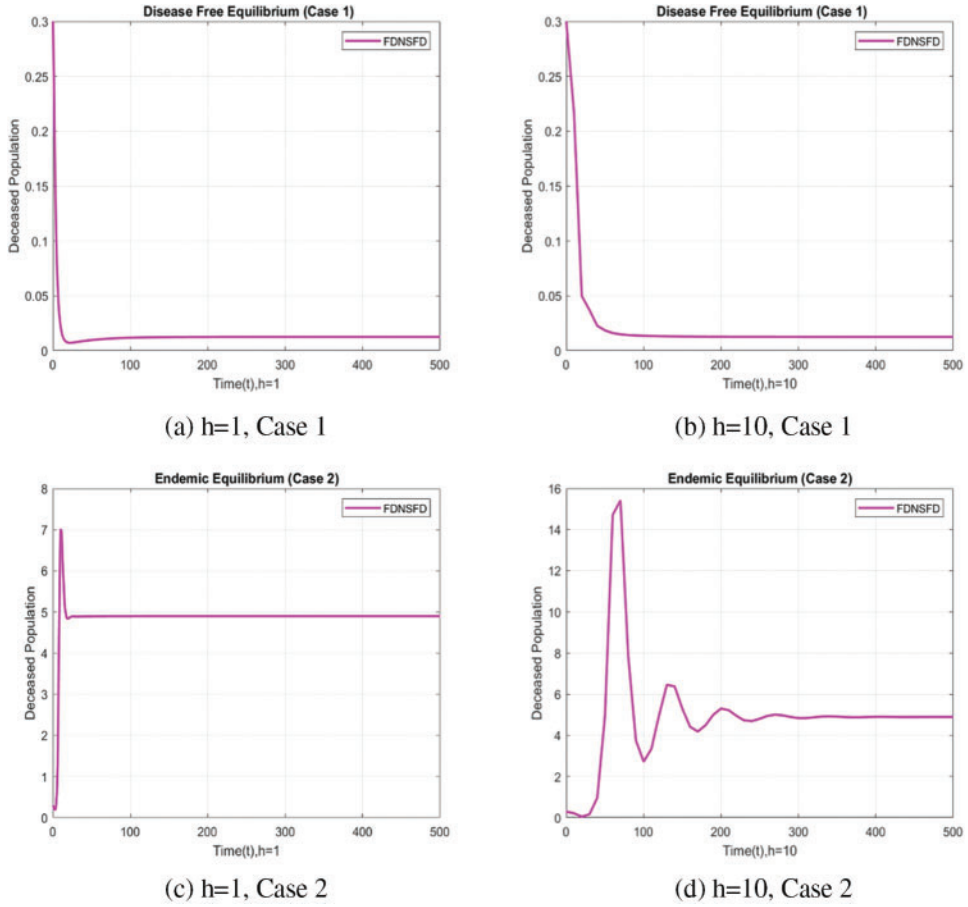

(a) h=1, Case 1 (b) h=10, Case 1

(c) h=1, Case 2 (d) h=10, Case 2

Figure 6: (Continued)

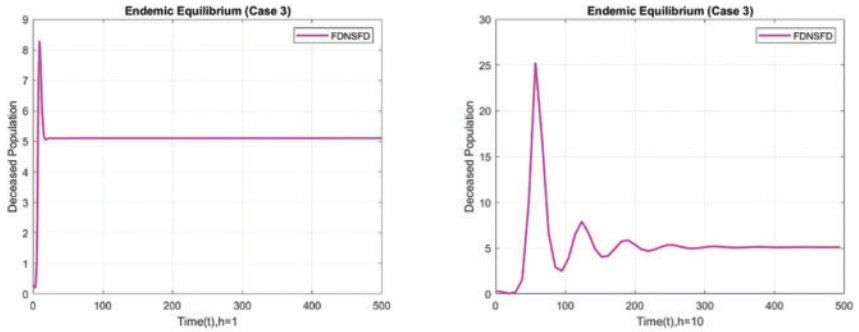

(e) h=1, Case 3 (f) h=10, Case 3

Figure 6: Deceased population at various step sizes using the FDNSFD approach

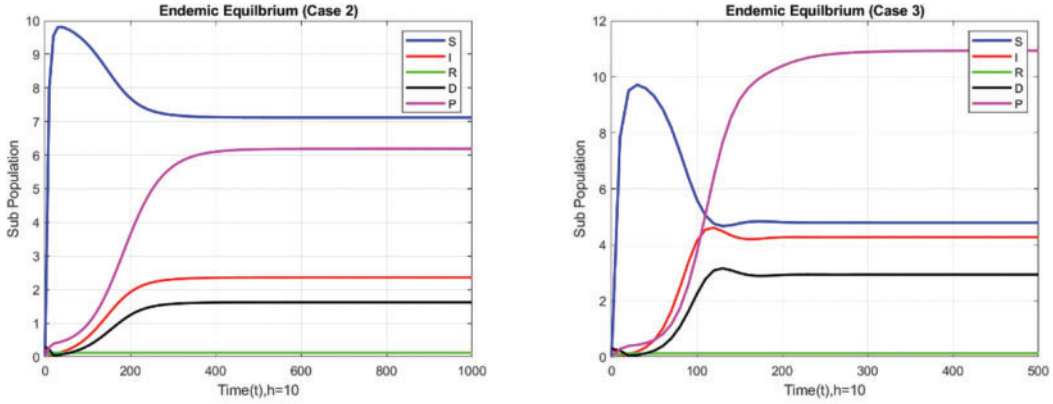

(a) h=10, Case 2 (b) h=10, Case 3

Figure 7: Compartmental comparison of SIRDP using the FDNSFD approach

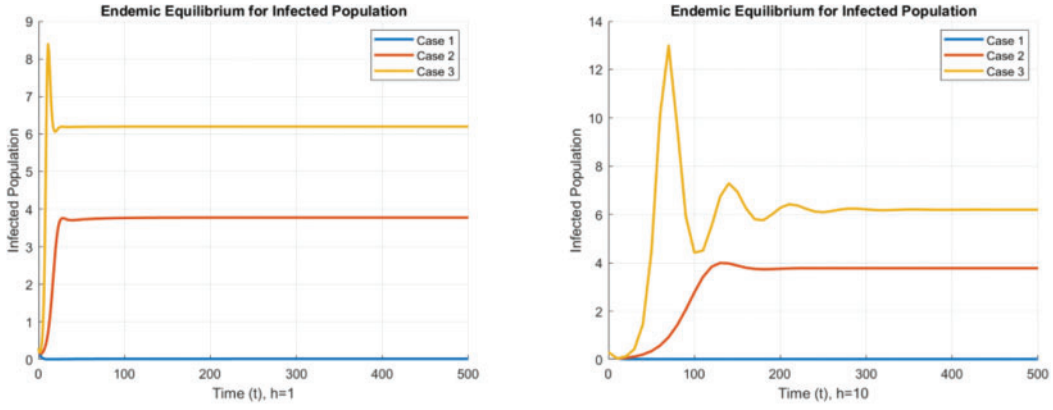

(a) h=1 (b) h=10

Figure 8: Infected population in each case using the FDNSFD approach

Fig. 10 illustrates the effect of τ on the infected and deceased population while using the FDNSFD approach. Overall, the NSFD approach models population dynamics, delivering realistic and reliable results while avoiding the non-physical outcomes of the forward approach.

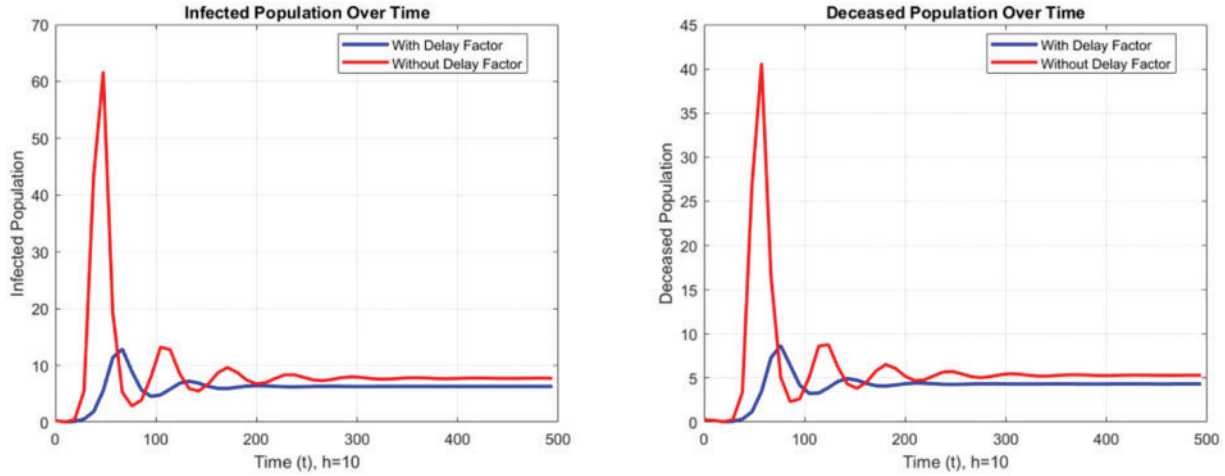

(a) infected population (b) deceased population

Figure 9: Effect of time delay on infected and deceased population using the FDNSFD approach

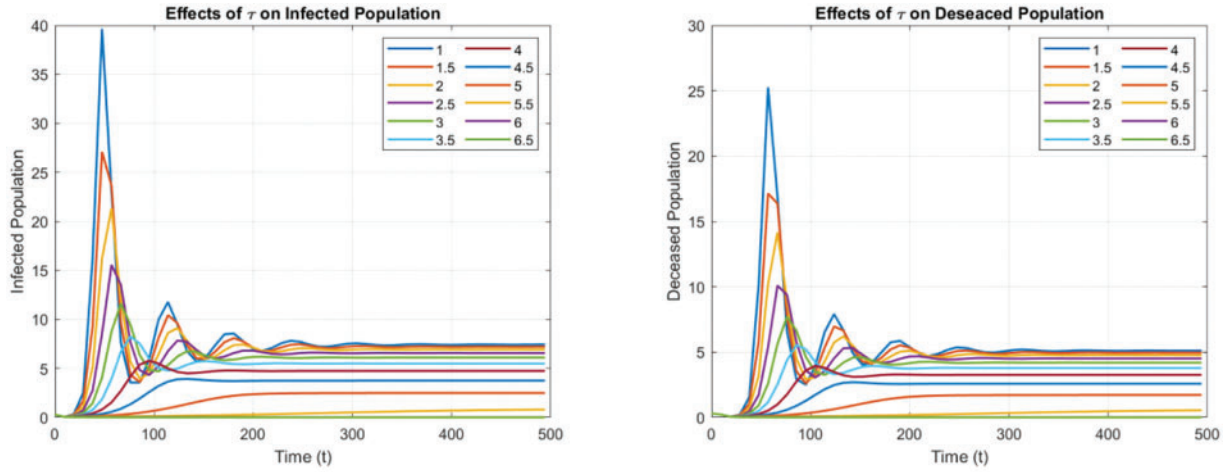

(a) effect on infected population (b) effect on deceased population

Figure 10: Effect of time delay τ on infected and deceased population

5 Conclusion

EVD still exists in the communities of Central and West Africa; hence, there is a need for models that can describe the transmission process accurately. Since the transmission dynamics and time effects of EVD are uncertain, the SIRDP epidemic model, which includes time delays and fuzzy parameters, was used. The forward Euler scheme and the FDNSFD scheme carried out simulations of the model. Comparing results obtained from the forward Euler method with those obtained from the

FDNSFD scheme, it was evident that though the forward Euler method is quite popular, the FDNSFD scheme was found to be more capable of preserving properties like positivity, stability, and accuracy, which makes it a competent tool for investigating the spread of EVD. This was also demonstrated in that adding the time delay facilitates halting disease spread by anticipating the delayed effects on transmission. As stated previously, the FDNSFD strategy can be concluded to have been utilizing EVD trends and may help the regulatory agencies in the future control of EVD transmission.

Despite these contributions, the study has several limitations. Thus, the quality of the epidemiological data influences the study and depends on the reporting system, which could be inconsistent. Some parts of Central and West Africa have the worst healthcare system; they rarely have enough resources to enable them to conduct an effective response to outbreaks. Isolation measures and vaccination campaigns are some of the public health strategies used to counter the epidemic disease, and their implementation differs across different regions, hence impacting transmission rates. Such assumptions as equal population distribution and equal transmission rates for contacts may not adequately give a full depiction of reality. The FDNSFD scheme may be constrained in some parameter domains, and the forward Euler method may add numerical errors. Further, the model is structured without regard to regional differences or other approaches, which reduces the scope for the application other than the Central and West African countries. These issues should be addressed in future work.

Acknowledgement: The authors Thabet Abdeljawad and Bahaaeldin Abdalla would like to thank Prince Sultan University for paying the APC and for the support through TAS research lab.

Funding Statement: The authors received no specific funding for this study.

Author Contributions: Conceptualization, methodology, software, and draft manuscript preparation: Muhammad Tashfeen and Fazal Dayan; Formal analysis, methodology, software, validation, and supervision: Muhammad Aziz ur Rehman, Thabet Abdeljawad and Bahaaeldin Abdalla. All authors reviewed the results and approved the final version of the manuscript.

Availability of Data and Materials: The data presented in this article are available from the corresponding author upon reasonable request.

Ethics Approval: Not applicable.

Conflicts of Interest: The authors declare no conflicts of interest to report regarding the present study.

References

1. Bernoulli D, Blower S. Attempt at a new analysis of mortality caused by smallpox and the advantages of inoculation to prevent it. HAL Open Sci. 2004;14(5):75–88.
2. Ross R. The prevention of malaria. London: John Murray; 1911.
3. Kermack WO, McKendrick AG. Contributions to the mathematical theory of epidemics–I. 1927. Bull Math Biol. 1991;53(1–2):33–55. doi:10.1007/BF02464423.
4. van den Driessche P, Watmough J. Reproduction numbers and sub-threshold endemic equilibria for compartmental models of disease transmission. Math Biosci. 2002;180(1–2):29–48. doi:10.1016/S0025-5564(02)00108-6.
5. En'Ko PD. On the course of epidemics of some infectious diseases. Int J Epidemiol. 1989;18(4):749–55. doi:10.1093/ije/18.4.749.
6. Brauer F, Castillo-Chavez C, Feng Z. Math model epid. New York: Springer; vol. 32, 2019.

7. Martin DL, Gustafson TL, Pelosi JW, Suarez LA, Pierce GV. Contaminated produce—a common source for two outbreaks of Shigella gastroenteritis. Am J Epidemiol. 1986 Aug 1;124(2):299–305. doi:10.1093/oxfordjournals.aje.a114388.
8. Swaddiwudhipong W, Karintraratana S, Kavinum S. A common-source outbreak of shigellosis involving a piped public water supply in northern Thai communities. J Trop Med Hyg. 1995;98:14550.
9. Hethcote HW. The mathematics of infectious diseases. SIAM Rev. 2000;42(4):599–653. doi:10.1137/S0036144500371907.
10. Misra AK, Sharma A, Shukla JB. Modeling and analysis of effects of awareness programs by media on the spread of infectious diseases. Math Comput Model. 2011;53(5–6):1221–8. doi:10.1016/j.mcm.2010.12.005.
11. Rihan FA. Delay differential equations and applications to biology. Singapore: Springer; 2021 Aug 19.
12. Smith HL. An introduction to delay differential equations with applications to the life sciences. New York: Springer; 2011.
13. Brauer F, Castillo-Chavez C. Mathematical models for communicable diseases. USA: SIAM; 2012
14. Meziane M, Moussaoui A, Volpert V. On a two-strain epidemic model involving delay equations. Math Biosci Eng. 2023;20(12):20683–711. doi:10.3934/mbe.2023915.
15. Ghosh S, Volpert V, Banerjee M. An epidemic model with time delay determined by the disease duration. Mathematics. 2022;10(15):2561. doi:10.3390/math10152561.
16. Almuqati BM, Allehiany FM. Global stability of a multi-group delayed epidemic model with logistic growth. AIMS Math. 2023;8(10):23046–61. doi:10.3934/math.20231173.
17. Beretta E, Hara T, Ma W, Takeuchi Y. Global asymptotic stability of an SIR epidemic model with distributed time delay. Nonlinear Anal. 2001;47(6):4107–15. doi:10.1016/S0362-546X(01)00528-4.
18. Ma Z. Dynamical modeling and analysis of epidemics. Singapore: World Scientific; 2009.
19. Tipsri S, Chinviriyasit W. The effect of time delay on the dynamics of an SEIR model with nonlinear incidence. Chaos Solit Fractals. 2015;75:153–72. doi:10.1016/j.chaos.2015.02.017.
20. Hussien RM, Naji RK. The dynamics of a delayed ecoepidemiological model with nonlinear incidence rate. J Appl Math. 2023;2023(1):1366763. doi:10.1155/2023/1366763.
21. Shatanawi W, Abdo MS, Abdulwasaa MA, Shah K, Panchal SK, Kawale SV, et al. A fractional dynamics of tuberculosis (TB) model in the frame of generalized Atangana-Baleanu derivative. Results Phys. 2021;29:104739. doi:10.1016/j.rinp.2021.104739.
22. Alkhazzan A, Wang J, Nie Y, Khan H, Alzabut J. A novel SIRS epidemic model for two diseases incorporating treatment functions, media coverage, and three types of noise. Chaos Solit Fractals. 2024;181:114631. doi:10.1016/j.chaos.2024.114631.
23. Aldwoah KA, Almalahi MA, Abdulwasaa MA, Shah K, Kawale SV, Awadalla M, et al. Mathematical analysis and numerical simulations of the piecewise dynamics model of Malaria transmission: a case study in Yemen. AIMS Math. 2024;9(2):4376–408. doi:10.3934/math.2024216.
24. Din A, Li Y, Yusuf A. Delayed hepatitis B epidemic model with stochastic analysis. Chaos Solitons Fractals. 2021;146:110839. doi:10.1016/j.chaos.2021.110839.
25. Din A. Bifurcation analysis of a delayed stochastic HBV epidemic model: cell-to-cell transmission. Chaos Solit Fractals. 2024;181:114714. doi:10.1016/j.chaos.2024.114714.
26. Zimmermann H-J. Fuzzy set theory—and applications. 4th ed. Boston: Kluwer Academic Publishers; 2001.
27. Bates JH, Young MP. Applying fuzzy logic to medical decision making in the intensive care unit. Am J Respir Crit Care Med. 2003;167(7):948–52. doi:10.1164/rccm.200207-777CP.
28. Abdy M, Side S, Annas S, Nur W, Sanusi W. An SIR epidemic model for COVID-19 spread with fuzzy parameter: the case of Indonesia. Adv Differ Equ. 2021;2021(1):1–7. doi:10.1186/s13662-021-03263-6.
29. Li C, Huang J, Chen YH, Zhao H. A fuzzy susceptible-exposed-infected-recovered model based on the confidence index. Int J Fuzzy Syst. 2021;23:907–17.

30. Shi X, Li J, Huang A, Song S, Yang Z. Assessing the outbreak risk of epidemics using fuzzy evidential reasoning. Risk Anal. 2021;41(11):2046–64. doi:10.1111/risa.13730.
31. Stiegelmeier EW, Bressan GM. A fuzzy approach in the study of COVID-19 pandemic in Brazil. Res Biomed Eng. 2021;37(2):263–71. doi:10.1007/s42600-021-00144-5.
32. Dayan F, Ahmed N, Rafiq M, Iqbal MS, Khan I, Raza A, et al. A dynamically consistent approximation for an epidemic model with fuzzy parameters. Expert Syst Appl. 2022;210(6):118066. doi:10.1016/j.eswa.2022.118066.
33. Alqarni MM, Rafiq M, Dayan F, Awrejcewicz J, Ahmed N, Raza A, et al. New trends in fuzzy modeling through numerical techniques. Comput Mater Contin. 2023;74(3):6371–88. doi:10.32604/cmc.2023.033553.
34. Baseler L, Chertow DS, Johnson KM, Feldmann H, Morens DM. The pathogenesis of Ebola virus disease. Annu Rev Pathol. 2017 Jan 24;12(1):387–418.
35. Sullivan NJ, Sanchez A, Rollin PE, Yang ZY, Nabel GJ. Development of a preventive vaccine for Ebola virus infection in primates. Nature. 2000;408(6812):605–9. doi:10.1038/35046108.
36. World Health Organization. Ebola virus disease. Available from: https://www.who.int/news-room/fact-sheets/detail/ebola-virus-disease. [Accessed 2024 Jul 15].
37. Malik S, Kishore S, Nag S, Dhasmana A, Preetam S, Mitra O, et al. Ebola virus disease vaccines: development, current perspectives & challenges. Vaccine. 2023;11(2):268. doi:10.3390/vaccines11020268.
38. Area I, Batarfi H, Losada J, Nieto JJ, Shammakh W, Torres Á. On a fractional order Ebola epidemic model. Adv Differ Equ. 2015;2015(1):1–2. doi:10.1186/s13662-015-0613-5.
39. Rachah A, Torres DF. Predicting and controlling the Ebola infection. Math Methods Appl Sci. 2017;40(17):6155–64. doi:10.1002/mma.3841.
40. Ismail S, Mtunya AP. A mathematical analysis of an in-vivo ebola virus transmission dynamics model. Tanz J Sci. 2021;47(4):1464–77. doi:10.4314/tjs.v47i4.12.
41. Rachah A, Torres DF. Mathematical modelling, simulation, and optimal control of the 2014 Ebola outbreak in West Africa. Discrete Dyn Nat Soc. 2016;2016:1–16. doi:10.1155/2016/1230758.
42. Webb G, Browne C, Huo X, Seydi O, Seydi M, Magal P. A model of the 2014 Ebola epidemic in West Africa with contact tracing. PLoS Curr. 2015 Jan 30;7. doi:10.1371/currents.
43. Nazir A, Ahmed N, Khan U, Mohyud-Din ST, Nisar KS, Khan I. An advanced version of a conformable mathematical model of Ebola virus disease in Africa. Alex Eng J. 2020;59(5):3261–8. doi:10.1016/j.aej.2020.08.050.
44. Verma R, Tiwari SP, Upadhyay RK. Transmission dynamics of epidemic spread and outbreak of Ebola in West Africa: fuzzy modeling and simulation. J Appl Math Comput. 2019;60(1–2):637–71. doi:10.1007/s12190-018-01231-0.
45. Ren H, Xu R. Prevention and control of Ebola virus transmission: mathematical modelling and data fitting. J Math Biol. 2024;89(2):25. doi:10.1007/s00285-024-02122-8.
46. Nisar KS, Farman M, Jamil K, Akgul A, Jamil S. Computational and stability analysis of Ebola virus epidemic model with piecewise hybrid fractional operator. PLoS One. 2024;19(4):e0298620. doi:10.1371/journal.pone.0298620.
47. Kengne JN, Tadmon C. Ebola virus disease model with a nonlinear incidence rate and density-dependent treatment. Infect Dis Model. 2024;9(3):775–804. doi:10.1016/j.idm.2024.03.007.
48. Abbas N, Zanib SA, Ramzan S, Nazir A, Shatanawi W. A conformable mathematical model of Ebola virus disease and its stability analysis. Heliyon. 2024;10(16):e35818. doi:10.1016/j.heliyon.2024.e35818.
49. Ko Y, Lee J, Seo Y, Jung E. A comprehensive analysis of non-pharmaceutical interventions and vaccination on Ebolavirus disease outbreak: stochastic modeling approach. PLoS Negl Trop Dis. 2024;18(6):e0011955. doi:10.1371/journal.pntd.0011955.
50. Xu C, Farman M. Dynamical transmission and mathematical analysis of Ebola virus using a constant proportional operator with a power law kernel. Fractals. 2023;7(10):706. doi:10.3390/fractalfract7100706.

51. Rosa S, Ndaïrou F. Optimal control applied to piecewise-fractional Ebola model. Mathematics. 2024;12(7):985. doi:10.3390/math12070985.
52. Mhlanga A. Assessing the impact of optimal health education programs on the control of zoonotic diseases. Comput Math Methods Med. 2020;2020(1):6584323. doi:10.32604/cmes.2023.028239.
53. Ahmad W, Abbas M. Effect of quarantine on transmission dynamics of Ebola virus epidemic: a mathematical analysis. Eur PhysJ Plus. 2021;136(4):1–33. doi:10.1140/epjp/s13360-021-01360-9.
54. Djiomba Njankou SD, Nyabadza F. Modelling the role of human behaviour in Ebola virus disease (EVD) transmission dynamics. Comput Math Methods Med. 2022;2022(1):4150043. doi:10.1155/2022/4150043.
55. Noorwali M, Shagari MS. On fractional differential inclusion for an epidemic model via L-fuzzy fixed point results. Comput Model Eng Sci. 2023;137(2):1937–56. doi:10.32604/cmes.2023.028239.
56. Alazman I, Albalawi KS, Goswami P, Malik K. A restricted SIR model with vaccination effect for the epidemic outbreaks concerning COVID-19. Comput Model Eng Sci. 2023;137(3):2409–2425. doi:10.32604/cmes.2023.028674.
57. Berge T, Lubuma JS, Moremedi GM, Morris N, Kondera-Shava R. A simple mathematical model for Ebola in Africa. J Biol Dyn. 2017;11(1):42–74. doi:10.1080/17513758.2016.1229817.
58. Bhuju G, Phaijoo GR, Gurung DB. Fuzzy approach analyzing SEIR-SEI dengue dynamics. Biomed Res Int. 2020;2020(1):1508613. doi:10.1155/2020/1508613.
59. Mangongo YT, Bukweli JD, Kampempe JD. Fuzzy global stability analysis of the dynamics of malaria with fuzzy transmission and recovery rates. Am J Oper Res. 2021;11(6):257–82. doi:10.4236/ajor.2021.116017.
60. Chitnis N, Hyman JM, Cushing JM. Determining important parameters in the spread of malaria through the sensitivity analysis of a mathematical model. Bull Math Biol. 2008;70(5):1272–96. doi:10.1007/s11538-008-9299-0.
61. Alsaadi A, Dayan F, Ahmed N, Baleanu D, Rafiq M, Raza A. Evolutionary computational method for tuberculosis model with fuzziness. AIP Adv. 2023;13(8):85125. doi:10.1063/5.0165348.